Depletion of horizontal pair diffusion in strongly stratified turbulence: Comparison with plane two-dimensional flows

F. Nicolleau*
The University of Sheffield, Department of Mechanical Engineering, Mapping Street, Sheffield, S1 3JD, United Kingdom

K.-S. Sung and J. C. Vassilicos†
Imperial College London, Department of Aeronautics, Prince Consort Road, SW7 2BY, United Kingdom

(Received 15 April 2008; published 9 October 2008)

In this paper different arguments are put forward to explain why two-particle diffusion is depleted in the direction of stratification of a stably stratified turbulence. Kinematic simulations (KSs) which reproduce that depletion are used to shed light on the responsible mechanisms. The local horizontal divergence is studied and comparisons are made with two-dimensional kinematic simulation. The probability density function of the horizontal divergence of the velocity field is not a Dirac distribution in the presence of stratification but a Gaussian and this Gaussian does not depend on the Froude number. The number of stagnation points in the KS of three-dimensional strongly stratified turbulence is found virtually identical to what it is in KS of three-dimensional isotropic turbulence. However, the root mean square horizontal and vertical stagnation point velocities of the stratified turbulence are both larger than their counterparts in isotropic turbulence that latter getting progressively smaller as the Reynolds number increases. Therefore, the strong stratification destroys the persistence of the stagnation points. The main reason for the depletion, however, seems to have to be sought in the effect of stratification on the strain rate tensor. The stratification does lead to a depletion of the average square strain rate tensor, as well as of all average square strain rate eigenvalues. We conclude that it is these effects of stratification on the strain rate tensor that explain the depletion of the horizontal turbulent pair diffusion.

DOI: 10.1103/PhysRevE.78.046306 PACS number(s): 47.27.eb, 47.55.Hd

I. INTRODUCTION

Stratification can be found in many geophysical or industrial flows (e.g., diffusion of pollutants in the atmosphere or ocean, movement and growth of clouds). The term "stratified flow" is normally used for "flow of stratified fluid" or, more precisely, "density stratified fluid," and this is the meaning it has in this paper. In these fluids, the density varies with the position in the fluid, and this variation is important in terms of fluid dynamics. Normally, the density variation is stable with nearly horizontal lines of constant density, i.e., lighter fluid above and heavier fluid below. The density variation may be continuous, as it occurs in most of the atmosphere and oceans, this is the case we consider in this paper, meaning a fluid with a negative density gradient in the vertical direction. In many situations the variation of density is very small. However, this small variation can have a severe effect on the flow if the small buoyancy forces can come into play.

One particle diffusion [10] in stratified flow has already received much attention [2–5]. In this paper, we focus on pair particle diffusion of fluid elements in stratified turbulence.

The pair particle mean square displacement $\Delta^2(t)$ is defined as

$$\Delta^2(t) = \left\langle \sum_{i=1,3} \{x_i^{(2)}(t) - x_i^{(1)}(t)\}^2 \right\rangle, \tag{1}$$

where i is the ith component of the particle position vector $\mathbf{x}$. $\mathbf{x}^{(1)}$ and $\mathbf{x}^{(2)}$ refer, respectively, to the first and second particle and $\langle \cdots \rangle$ represents the ensemble average.

Richardson [6] stated that the turbulent diffusivity $(d/dt)\Delta^2(t)$ at time t is mainly governed by the eddies of size $\Delta(t)$. It is that hypothesis, that we refer to as the locality assumption, that leads to the four-third law of diffusion

$$\frac{d}{dt}\langle \Delta^2(t) \rangle = 3G_\Delta{}^{1/3}\epsilon^{1/3}\Delta'(t)^{4/3}, \tag{2}$$

where $\Delta'(t) = \langle \Delta^2(t) \rangle^{1/2}$, ϵ is the turbulence kinetic energy dissipation rate per unit mass, and G_Δ a universal dimensionless constant called Richardson constant.

Richardson's locality assumption can be studied by estimating Richardson's coefficient β defined as follows:

$$\beta = \frac{3G_\Delta^{1/3}\epsilon^{1/3}}{u'/L^{1/3}} \tag{3}$$

[7,8]. In this paper we propose to use kinematic simulations (KSs) in order to understand better the turbulent diffusivity properties in the direction of stratification. KSs have demonstrated their ability to reproduce turbulent pair diffusion with Richardson's scaling both for isotropic turbulence [9] and for stably stratified turbulence in the horizontal plane [8,11,12]. This scaling is clear evidence of the turbulent diffusivity's dependence on the pair separation.

*F.Nicolleau@Sheffield.ac.uk
†j.c.vassilicos@imperial.ac.uk

It is well known that stratification decreases the vertical diffusion. Reference [7] also showed that stratification causes a decrease of the pair diffusion in the horizontal plane. They measured this effect of stratification on the coefficient β. In this paper we proposed different mechanisms in terms of stagnation points distribution and straining rates to explain their results and why β with stratification is smaller than its counterpart in two-dimensional KS and independent of the strength of the stratification.

II. NUMERICAL MODELS

A. Kinematic simulation (KS)

Kinematic simulations were first developed for incompressible isotropic turbulence where incompressibility and an energy power law spectrum are prescribed [13]. This model is based on a kinematically simulated Eulerian velocity field which is generated as a sum of random incompressible Fourier modes. This velocity field has a turbulentlike flow structure, that is eddying, straining and streaming regions, in every realization of the Eulerian velocity field, and the Lagrangian statistics are obtained by integrating individual particle trajectories in many realizations of this velocity field.

B. Boussinesq approximation

More details on the use of KS for one and two-particle diffusion in stably stratified nondecaying turbulence can be found in Refs. [3,4,8,11,12]. The KS model used here is based on the Boussinesq approximation. A stably stratified turbulence is given at static equilibrium, with pressure $p(x_3)$ and density $\rho(x_3)$ varying only along the vertical axis, that is in the direction of stratification. Hence, we have $dp/dx_3=-\rho g$, where $\mathbf{g}=(0,0,-g)$ is the gravity. For a stable stratification, the mean density gradient is negative, i.e., $d\rho/dx_3<0$ as the tilting of a density surface will produce a restoring force. From the Boussinesq approximation we have

$$\frac{D}{Dt}\left(\frac{\rho'}{\rho}\right)=-u_3\frac{1}{\rho}\frac{d\rho}{dx_3}, \tag{4}$$

where $D/Dt=\partial/\partial t+\mathbf{u}\cdot\boldsymbol{\nabla}$ is the derivative following the fluid particle, p' the perturbation pressure, and ρ' the density fluctuation, this latter is much smaller than ρ ($\rho'\ll\rho$) so that, in the limit of a vanishing viscosity, the dynamic equation becomes

$$\frac{D}{Dt}\mathbf{u}=-\frac{1}{\rho}\boldsymbol{\nabla}p'+\frac{\rho'}{\rho}\mathbf{g}. \tag{5}$$

The perturbation velocity $\mathbf{u}(x,t)=(u_1,u_2,u_3)$ is taken incompressible

$$\boldsymbol{\nabla}\cdot\mathbf{u}=0. \tag{6}$$

C. Linearized Boussinesq equations

The initial velocity $\mathbf{u}(\mathbf{x},0)$ can involve a large range of length scales, the smallest of these length-scale is η, the Kolmogorov length scale. In the limit where nonlinear terms can be neglected, that is when the micro-scale Froude number is much smaller than 1, i.e., $\mathrm{Fr}_\eta=u(\eta)/\mathcal{N}\eta\ll 1$, where $\mathcal{N}$ is the buoyancy (Brünt-Väissälä) frequency and $u(\eta)$ the characteristic velocity fluctuation at the Kolmogorov scale, the nonlinear terms in Eqs. (4) and (5) can be neglected which leads to the linearized Boussinesq equations

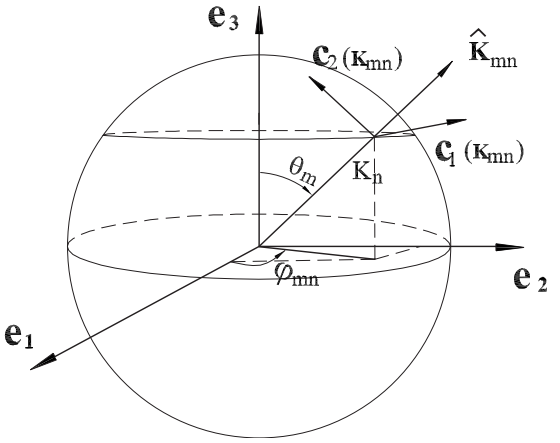

FIG. 1. Craya-Herring frame.

$$\frac{\partial\Theta}{\partial t}=-u_3\frac{1}{\rho}\frac{d\rho}{dx_3}, \tag{7}$$

$$\frac{\partial}{\partial t}\mathbf{u}=-\frac{1}{\rho}\boldsymbol{\nabla}p'+\Theta\mathbf{g}. \tag{8}$$

The Fourier transform $\tilde{\mathbf{u}}(\mathbf{k},t)$ of $\mathbf{u}(\mathbf{x},t)$ is used to solve Eqs. (7) and (8), so that the incompressibility requirement is transformed into $\mathbf{k}\cdot\tilde{\mathbf{u}}(\mathbf{k},t)=0$. If e_3 is the unit vector in the direction of stratification and e_1,e_2 two unit vectors normal to each other and to e_3 (so that $\mathbf{x}=x_1\mathbf{e}_1+x_2\mathbf{e}_2+x_3\mathbf{e}_3$ and $\mathbf{g}=-g\mathbf{e}_3$), the Craya-Herring frame (see Fig. 1) is given by the unit vector $\hat{\mathbf{k}}=\mathbf{k}/k$ and $\mathbf{c}_1=\mathbf{e}_3\times\mathbf{k}/|\mathbf{e}_3\times\mathbf{k}|$, $\mathbf{c}_2=\mathbf{k}\times\mathbf{c}_1/|\mathbf{k}\times\mathbf{c}_1|$. In the Craya-Herring frame the Fourier transformed velocity field $\tilde{\mathbf{u}}(\mathbf{k},t)$ lies in the plane defined by $\mathbf{c}_1$ and $\mathbf{c}_2$, i.e.,

$$\tilde{\mathbf{u}}(\mathbf{k},t)=\tilde{v}_1(\mathbf{k},t)\mathbf{c}_1+\tilde{v}_2(\mathbf{k},t)\mathbf{c}_2. \tag{9}$$

Incompressible solutions of Eqs. (7) and (8) in Fourier space and in the Craya-Herring frame are [14]

$$\tilde{v}_1(\mathbf{k},t)=\tilde{v}_1(\mathbf{k},0), \tag{10}$$

$$\tilde{v}_2(\mathbf{k},t)=\tilde{v}_2(\mathbf{k},0)\cos\sigma t-\frac{g}{\mathcal{N}}\tilde{\Theta}(\mathbf{k},0)\sin\sigma t, \tag{11}$$

$$\tilde{\Theta}(\mathbf{k},t)=\tilde{\Theta}(\mathbf{k},0)\cos\sigma t+\frac{\mathcal{N}}{g}\tilde{v}_2(\mathbf{k},0)\sin\sigma t, \tag{12}$$

where $\theta=\theta(\mathbf{k})$ is the angle between $\mathbf{k}$ and vertical axis $\mathbf{e}_3$ and $\sigma=\mathcal{N}\sin\theta$. The initial conditions that we choose are $\tilde{v}_1(\mathbf{k},0)$, $\tilde{v}_2(\mathbf{k},0)$, and $\tilde{\Theta}(\mathbf{k},0)=0$ (zero initial potential), then Eqs. (10)–(12) become

$$\tilde{v}_1(\mathbf{k},t)=\tilde{v}_1(\mathbf{k},0), \tag{13}$$

$$\tilde{v}_2(\mathbf{k},t) = \tilde{v}_2(\mathbf{k},0)\cos\sigma t, \tag{14}$$

$$\tilde{\Theta}(\mathbf{k},t) = \frac{\mathcal{N}}{g}\tilde{v}_2(\mathbf{k},0)\sin\sigma t. \tag{15}$$

We emphasize again that the linearized Boussinesq equations are valid for $\mathrm{Fr} \ll 1$ only.

D. Kinematic simulation of stratified with or without rotating turbulence

The initial three-dimensional turbulent field onto which the stable stratification is superimposed is an isotropic KS field (see, e.g., Ref. [4]):

$$\mathbf{u}(\mathbf{x},0) = 2\pi \sum_{n-1}^{N}\sum_{m=1}^{M} \tilde{\mathbf{u}}(\mathbf{k}_{mn},0)k_n^2 \sin\theta_m \Delta k_n \Delta\theta_m e^{i\mathbf{k}_{mn}\cdot\mathbf{x}} \tag{16}$$

and

$$\tilde{\mathbf{u}}(\mathbf{k}_{mn},0) = \tilde{v}_1(\mathbf{k}_{mn},0)\mathbf{c}_1(\mathbf{k}_{mn},0) + \tilde{v}_2(\mathbf{k}_{mn},0)\mathbf{c}_2(\mathbf{k}_{mn}), \tag{17}$$

where $\mathbf{k}_{mn}=k_n(\sin\theta_m\cos\phi_{nm}, \sin\theta_m \sin\phi_{nm}, \cos\theta_m)$. Note that $\mathbf{u}(\mathbf{x},0)$ is three dimensional and incompressible by construction because it is appropriately distributed in the Craya-Herring frame. $\tilde{v}_1(\mathbf{k}_{mn},0)$, $\tilde{v}_2(\mathbf{k}_{mn},0)$ are the decomposition of the Fourier transformed initial isotropic velocity field $\tilde{\mathbf{u}}(\mathbf{k}_{mn},0)$ in the Craya-Herring frame. It is worth remembering here the assumptions underlying Eqs. (16) and (17). Equation (16) is the classical KS decomposition in Fourier modes, whereas $\tilde{v}_1$ and $\tilde{v}_2$ are a rapid distortion theory (RDT) solution of the Boussinesq equation. As such this solution is valid when the linearization is valid, that is when the stratification is strong enough for its effects to be the fastest to develop. This has to be the case at all scales involved in turbulence. Therefore the validity criteria is a Froude number based on the Kolmogorov scale smaller than one (see, e.g., Ref. [3]).

The energy spectrum $E(k)$ is prescribed as follows:

$$\begin{cases} E(k) = E_0 L(kL)^4 & \text{for } 0 < k \leqslant k_L, \\ E(k) = E_0 L(kL)^{-5/3} & \text{for } k_L < k \leqslant k_n, \\ E(k) = 0 & \text{for } k_N < k, \end{cases} \tag{18}$$

$k_L=1/L$, where $L/2\pi$ is the energy containing length scale where the energy spectrum reaches its maximum value, E_0 is a characteristic energy, and the Kolmogorov length scale is defined as $\eta=1/k_N$. The wave number is geometrically distributed, i.e.,

$$k_n = k_1\left(\frac{k_N}{k_1}\right)^{(n-1)/(N-1)} \quad \text{and} \quad k_1 = \frac{1}{4L}. \tag{19}$$

Δk_n is then derived as

$$\Delta k_n = \frac{k_n}{N-1}\ln\left(\frac{k_N}{k_1}\right)\Delta n. \tag{20}$$

In order to capture correctly the effect of stratification, for each wave number, M wave vectors are defined such that

$$\theta_m = \frac{(m-1)}{M-1}\pi \quad \text{for} \quad 1 \leqslant m \leqslant M \tag{21}$$

and

$$\Delta\theta_m = \frac{\pi}{M-1}\Delta m. \tag{22}$$

Then, the angle in the horizontal plan φ_{mn} is chosen randomly in the range $[0,2\pi[$. From Eqs. (16) and (17), the velocity field $\mathbf{u}(\mathbf{x},t)$ can be expressed at any time as

$$\mathbf{u}(\mathbf{x},t) = 2\pi\,\mathrm{Re}\left\{\sum_{n-1}^{N}\sum_{m=1}^{M} k_n^2 \sin\theta_m \Delta k_n \Delta\theta_m e^{(i\mathbf{k}_{mn}\cdot\mathbf{x}+\omega_{mn}t)} \times [\tilde{v}_1(\mathbf{k}_{mn},t)\mathbf{c}_1(\mathbf{k}_{mn},t) + \tilde{v}_2(\mathbf{k}_{mn},t)\mathbf{c}_2(\mathbf{k}_{mn})]\right\}, \tag{23}$$

where "Re" stands for real part. $\tilde{v}_1(\mathbf{k}_{mn},t)$ and $\tilde{v}_2(\mathbf{k}_{mn},t)$ obey Eqs. (13) and (14), respectively. A time dependence $\omega_{mn}t$ has also been introduced in Eq. (23) in order to simulate time decorrelation within the Fourier modes [4]. $\omega_{mn}=\lambda_{mn}\sqrt{k_n^3 E(k_n)}$, where λ_{mn} is a dimensionless unsteadiness coefficient equal to 0.5 for all m and n in this paper.

In order to calculate the particles' diffusion, we track the particles in time using

$$\dot{\mathbf{x}}(t) = \mathbf{u}[\mathbf{x}(t),t]. \tag{24}$$

We obtain the Lagrangian trajectories $\mathbf{x}(t)$ by integrating Eq. (24) using Eq. (23) for the Eulerian velocity. Each particle is released at a time t_0 from an initial position x_0 randomly chosen in each realization.

III. DEPLETION OF HORIZONTAL PAIR DIFFUSION IN STRONGLY STRATIFIED TURBULENCE

If we consider the horizontal displacement only, we can look for a two-dimensional version of Eq. (2) as follows:

$$\frac{d}{dt}\langle\Delta_h^2(t)\rangle = 3G_{\Delta h}{}^{1/3}\epsilon^{1/3}\Delta_h'(t)^{4/3}, \tag{25}$$

where $\Delta_h'(t)=\sqrt{\langle\Delta_h^2(t)\rangle}$ is the r.m.s of the horizontal separation $\langle\Delta_h^2(t)\rangle$ which is defined as $\Sigma_{i=1}^2\langle\{x_i^{(2)}(t)-x_i^{(1)}(t)\}^2\rangle$ where the superscripts (1) and (2) refer to particles (1) and (2); $i=1,2$ are coordinate subscripts in the horizontal plane. Using $\epsilon\sim u'^3/L$, where ϵ is the energy dissipation rate, we can define the constant β_h as

$$\beta_h = \frac{3G_{\Delta h}^{1/3}\epsilon^{1/3}}{u'/L^{1/3}} \tag{26}$$

and therefore write

$$\frac{d}{dt}\langle\Delta_h^2(t)\rangle = \beta_h u'\,\eta\left(\frac{L}{\eta}\right)^{-1/3}\left(\frac{\Delta_h'(t)}{\eta}\right)^{4/3}, \tag{27}$$

where L and η are, respectively, the energy containing length scale and the Kolmogorov length scale.

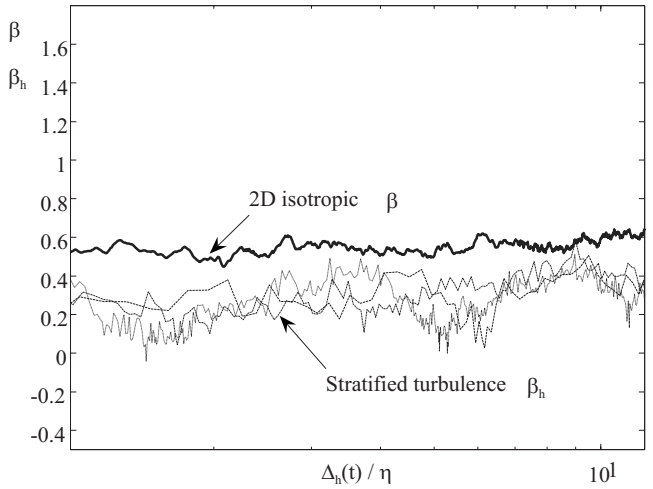

FIG. 2. β_h as a function of $\Delta_h(t)/\eta$ for $\mathcal{N}=500$, 1250, and 2500. Cases A, B, C, and D (isotropic) in Table I.

Reference [7] compared β_h of stratified turbulence with β_h of three-dimensional isotropic incompressible turbulence and found that β_h does not depend on the strength of the buoyancy. For a more precise comparison, here β_{2D} of two-dimensional isotropic incompressible turbulence is also computed and compared with β_h [β_{2D} is also defined by Eq. (27) but for a two-dimensional flow]. Values of β_h for stratified turbulence as functions of $\Delta_h'(t)/\eta$ for different buoyancy frequencies $\mathcal{N}$ are presented in Fig. 2, where the two-dimensional isotropic KS turbulence case is also plotted for the sake of comparison.

Particle pairs are released at a random time $t_0=(10+\delta)2\pi/\mathcal{N}$, where δ is a random number between -1 and 1 different for each pair in order to avoid them oscillating in phase. This initial time is large enough for the velocities to have reached their anisotropic r.m.s values as a result of stratification's rapid distortion [4]. Averages are taken over 4 pairs in 250 realizations.

The coefficient β_h for purely stratified turbulence is calculated for Froude numbers Fr=0.0007, 0.00028, and 0.00014 (other simulation parameters are given in Table I) and the results are in good agreement with Refs. [11]. Figure 2 shows that when there is stratification β_h is reduced compared to the two-dimensional case while, as for the two-dimensional case, it remains almost independent of Δ_h/η, in the range $\eta \leqslant \Delta_h(t) \leqslant L$. Furthermore, within statistical accuracy, β_h is independent of $\mathcal{N}$ in this range.

We can therefore conclude following [11] that the horizontal locality-in-scale hypothesis which leads to Eq. (27) with $(d/dt)\beta_h=0$ remains valid in strongly and stably stratified turbulence but with a modified value of β_h which is independent of $\mathcal{N}$. We emphasize that the horizontal pair diffusion is depleted in the presence of stratification and this is not due to considering only two components of the displacement as we have compared $\beta_h(\mathcal{N})$ with two-dimensional turbulence and found

$$\beta_h(\mathcal{N} \neq 0) < \beta_{2D}. \tag{28}$$

The coefficient β_{2D} for a two-dimensional isotropic turbulence is smaller than its counterpart in three-dimensional isotropic turbulence (noted β_{3h}). In d-dimensional isotropic turbulence, pair separation is defined as $\langle\Delta^2\rangle=\langle\Delta_1^2\rangle+\cdots+\langle\Delta_d^2\rangle$ where $\Delta_i=x_i^{(2)}-x_i^{(1)}$ for $i=1$ to d. This can be rewritten as $\langle\Delta^2\rangle=d\langle\Delta_1^2\rangle$ in isotropic d-dimensional turbulence, so that from

$$\langle\Delta^2\rangle = G_{\Delta,2}\epsilon t^3 \tag{29}$$

in two-dimensional isotropic turbulence and

$$\langle\Delta^2\rangle = G_{\Delta,3}\epsilon t^3 \tag{30}$$

in three-dimensional isotropic turbulence, it follows that $G_{\Delta,3}/3=G_{\Delta,2}/2$, i.e.,

$$G_{\Delta,2} = \frac{2}{3}G_{\Delta,3} < G_{\Delta,3}. \tag{31}$$

Using Eq. (3), it follows that $\beta_{2D} < \beta_{3h}$.

IV. PROBABILITY DENSITY FUNCTION (pdf) OF HORIZONTAL VELOCITY DIVERGENCE IN STRATIFIED TURBULENCE

In Sec. III, we saw that β_h is not affected by the strength of the buoyancy and that it is also smaller than what it would be in isotropic incompressible turbulence. This indicates that the turbulent diffusivity is almost the same for any small enough Froude number when strong and stable stratification exists in a turbulent flow.

In a two-dimensional flow the incompressibility condition yields

$$\boldsymbol{\nabla}_h \cdot \mathbf{u}_h = \frac{\partial}{\partial x_1}u_1 + \frac{\partial}{\partial x_2}u_2 = 0. \tag{32}$$

Whereas, in the stratified flow, though $\langle u_3^2\rangle < \langle u_1^2\rangle = \langle u_2^2\rangle$, Eq. (32) is not true everywhere. To better understand the topological differences between the two-dimensional flow and the horizontal flow resulting from stratification we calculate

TABLE I. Different cases studied in Secs. III and IV.

Case		$\mathrm{Fr}=u'/L\mathcal{N}$	$\mathcal{N}$	L/η	u'	λ	Δ_0/η	L	$1/\eta$
A	stratified	0.0007	500	400	0.35	0.5	0.1	1	400
B	stratified	0.00028	1250	400	0.35	0.5	0.1	1	400
C	stratified	0.00014	2500	400	0.35	0.5	0.1	1	400
D	3D isotropic	∞	0	400	0.35	0.5	0.1	1	400
E	2D isotropic	∞	0	400	2	0.5	0.1	1	400

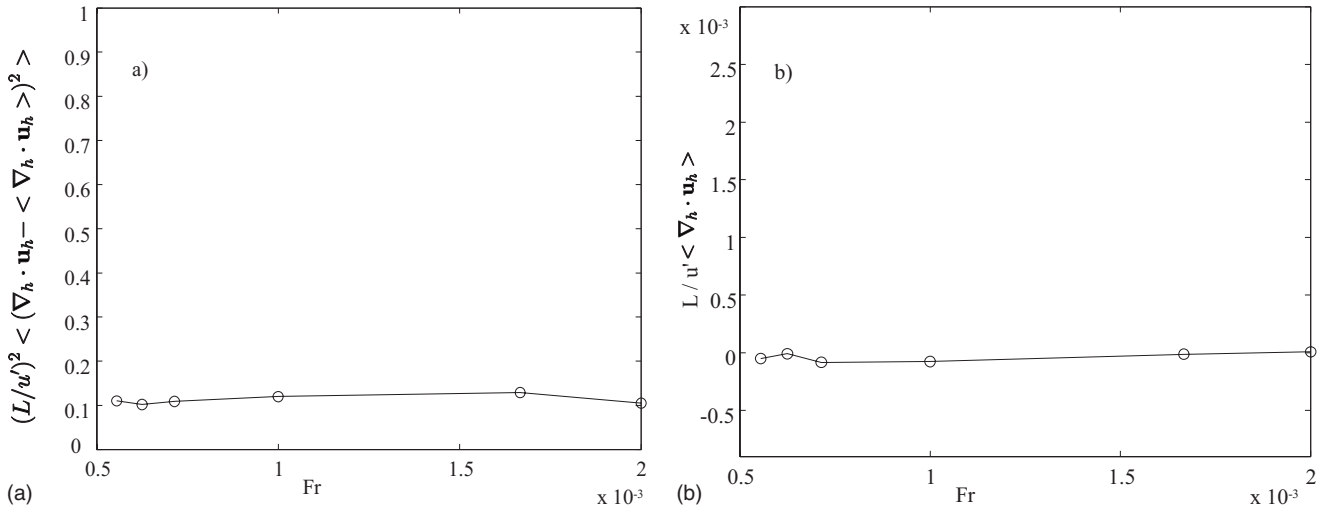

FIG. 3. (a) $(L/u')^2\langle(\boldsymbol{\nabla}_h\cdot\mathbf{u}_h-\langle\boldsymbol{\nabla}_h\cdot\mathbf{u}_h\rangle)^2\rangle$; (b) $\frac{L}{u'}\langle\boldsymbol{\nabla}_h\cdot\mathbf{u}_h\rangle$ as functions of the Froude number.

the probability density function of the horizontal velocity divergence

$$\boldsymbol{\nabla}_h \cdot \mathbf{u}_h = \frac{\partial}{\partial x_1}u_1 + \frac{\partial}{\partial x_2}u_2 \tag{33}$$

for the stratified flow. In particular, we compute the normalized mean

$$\frac{L}{u'}\langle\boldsymbol{\nabla}_h \cdot \mathbf{u}_h\rangle \tag{34}$$

and fluctuation variance

$$\left(\frac{L}{u'}\right)^2\langle(\boldsymbol{\nabla}_h \cdot \mathbf{u}_h - \langle\boldsymbol{\nabla}_h \cdot \mathbf{u}_h\rangle)^2\rangle \tag{35}$$

in order to compare the shape of the pdf of $\boldsymbol{\nabla}_h\cdot\mathbf{u}_h$ to a Gaussian distribution. The variation with the Froude number of these two statistics and pdf will help explaining why the strength of the buoyancy does not affect β_h and why depletion of horizontal pair diffusion exists. Figure 3 shows the normalized mean and variance of the horizontal velocity divergence as functions of the Froude number.

As expected the mean and variance values remain almost constant, showing no dependence of β_h on the Froude number. Thus, we can expect the probability density functions to have the same shapes for all Froude numbers. Furthermore, we may expect the pdf to be skewed towards negative values if horizontal compressibility is the reason for $\beta_h < \beta_{2D}$. Figure 4 shows that the pdf of the horizontal divergence of the stratified velocity field is not a Dirac distribution, as it would be for a two-dimensional turbulence, but a Gaussian centered on 0. However, this Gaussian pdf does not depend on the Froude number; this again is consistent with the result that β_h does not depend on the Froude number.

At this stage, it is still difficult to conclude whether this pdf can explain the depletion of horizontal pair diffusion because of the symmetrical Gaussian structure of this probability density function which implies equal probability for flow convergence (negative range of pdf) and flow divergence (positive range of pdf). This observation alone is therefore not sufficient to explain the depletion of horizontal turbulent pair diffusion. Therefore, more detailed results on the pair diffusion in isotropic nonincompressible turbulence are needed.

A. Modified two-dimensional isotropic kinematic simulation

In this section, we study the probability density function of the horizontal divergence in a two-dimensional KS where the incompressibility condition is artificially relaxed. This is done in order to understand the effect of compressibility on the depletion of horizontal pair diffusion.

Isotropic two-dimensional KS velocity fields are given by

$$\mathbf{u}(\mathbf{x},t) = \sum_{n=1}^{N} \mathbf{A}_n \cos(\mathbf{k}_n \cdot \mathbf{x} + \omega_n t) + \mathbf{B}_n \sin(\mathbf{k}_n \cdot \mathbf{x} + \omega_n t), \tag{36}$$

where N is the number of modes in the simulation, $\mathbf{k}_n = k_n\hat{\mathbf{k}}_n$, where $\hat{\mathbf{k}}_n$ is a random unit vector in the plane and $\mathbf{A}_n$ and $\mathbf{B}_n$ are vectors normal to $\hat{\mathbf{k}}_n$ in that plane. The amplitudes of these vectors are set by

$$E(k) = E_0 L(kL)^{-5/3} \tag{37}$$

and

$$|\mathbf{A}_n|^2 = |\mathbf{B}_n|^2 = E(k_n)\Delta k_n, \tag{38}$$

where $E_0 = \int_0^\infty E(k) = u'^2$, $\Delta k_n = k_{n+1} - k_n$ for $1 \leqslant n \leqslant N-1$ and $\Delta k_N = k_N - k_{N-1}$ and $L = 2\pi/k_1$ is the upper limit length scale of the inertial range.

The distribution of wavenumbers is algebraic, i.e.,

$$k_n = k_1\left(\frac{k_N}{k_1}\right)^{\ln n/\ln N}, \tag{39}$$

where $k_N = 2\pi/\eta$. The unsteadiness pulsation is $\omega_n = \lambda\sqrt{k_n^3 E(k_n)}$ where λ is a dimensionless constant ($\lambda = 0.5$ is used for this section's simulation).

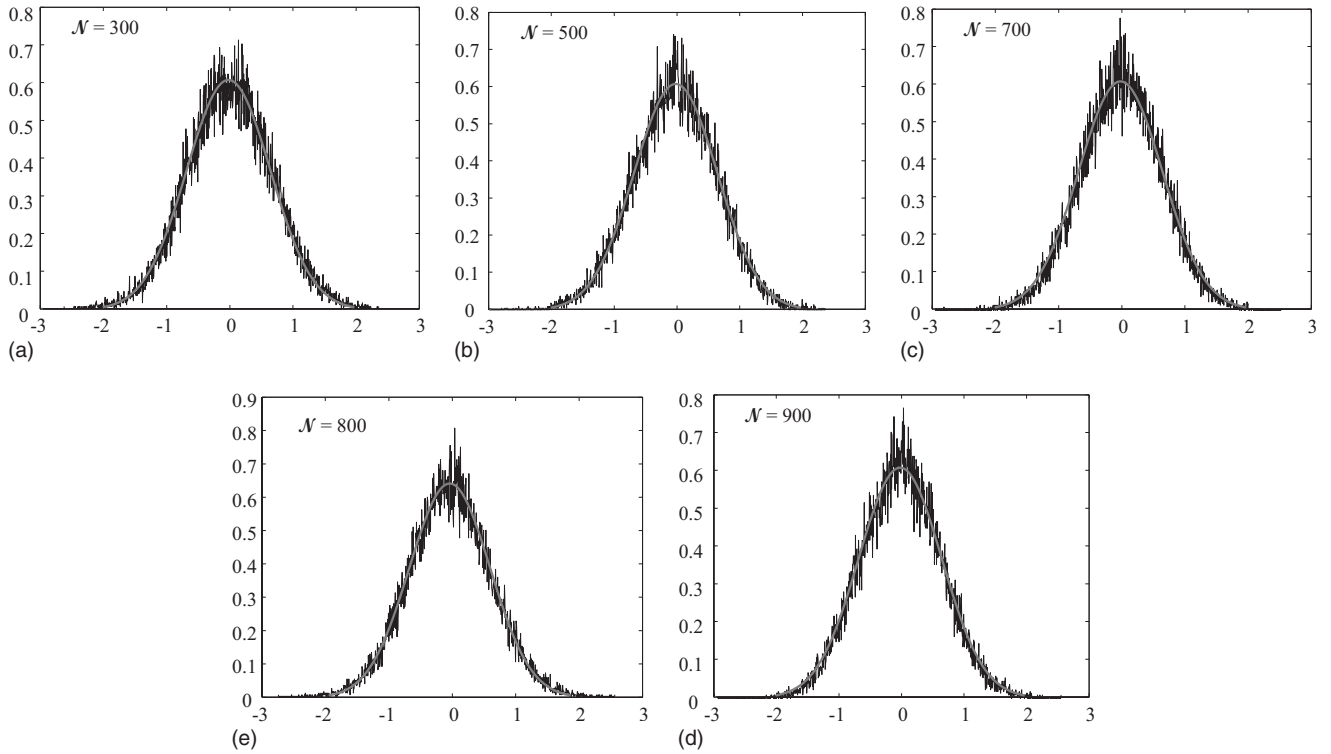

FIG. 4. PDF distributions of $(L/u')\nabla_h \cdot \mathbf{u}_h$ and their Gaussian fits (a) $\mathcal{N}=300$, (b) $\mathcal{N}=500$, (c) $\mathcal{N}=700$, (d) $\mathcal{N}=800$, (e) $\mathcal{N}=900$.

Flow parameters for the simulations in this section are $L=1$, $1/\eta=400$, $u'=2$, and $\Delta_0/\eta=0.1$, where Δ_0 is the initial separation of the two fluid particles. To insure incompressibility in kinematic simulation one imposes $\mathbf{A}_n \cdot \mathbf{k}_n = \mathbf{B}_n \cdot \mathbf{k}_n = 0$. By changing the angles between these vectors, the value of $\nabla \cdot \mathbf{u}$ can be modified to differ from 0. To do so, an angle ψ is introduced in the definition of $\mathbf{A}_n$, $\mathbf{B}_n$, and $\mathbf{k}_n$ for all n as follows:

$$\mathbf{A}_n = \begin{cases} -A_n \sin(\theta_n + \psi), \\ A_n \cos(\theta_n), \end{cases} \qquad \mathbf{B}_n = \begin{cases} B_n \sin(\theta_n), \\ -B_n \cos(\theta_n), \end{cases}$$

$$\mathbf{k}_n = \begin{cases} k_n \cos(\theta_n + \psi), \\ k_n \sin(\theta_n), \end{cases} \tag{40}$$

where ψ is chosen to be either π, $\pi/8$, or $\pi/16$. In this way, we break the orthogonality between $\mathbf{A}_n$ and $\mathbf{k}_n$ and between $\mathbf{B}_n$ and $\mathbf{k}_n$. When $\psi=0$, $\mathbf{A}_n \cdot \mathbf{k}_n = \mathbf{B}_n \cdot \mathbf{k}_n = 0$, and $\nabla \cdot \mathbf{u} = 0$. Figure 5 shows the probability density function of $\nabla \cdot \mathbf{u}$ in two-dimensional KS turbulence which is a Dirac distribution when $\psi=0$. Figure 6 shows the same pdf when $\psi \neq 0$, in this case it is clearly different from a Dirac distribution and it is also clear that this pdf gets broader with increasing ψ. Figure 7 shows what the effect of ψ is on β_{2D}. When ψ is a very small angle, i.e., $\psi=\pi/8$ and $\pi/16$, β_{2D} oscillates around the incompressible-KS value of β_{2D}, even though the probability density function of $\nabla \cdot \mathbf{u}$ (see Fig. 6) is much broader than that in Fig. 4. When $\psi=\pi$, the value of β_{2D} drops to a similar level as β_h for horizontal pair diffusion in strongly stratified KS turbulence.

If different flows have similar Richardson coefficients β, we may expect that they also have similar probability density functions of their velocity divergence. However, it is not the case: the pdf of the horizontal divergence in stably stratified turbulence in Fig. 4 is very different from that in Fig. 6.

The pdfs of horizontal velocity divergence can only partly explain the decrease of horizontal pair diffusion in stratified turbulence. The pdf of the horizontal velocity divergence in stably and strongly stratified turbulence is independent of the Froude number and also different from a Dirac distribution: it is a Gaussian with a zero mean and a standard deviation which scales as u'/L and is independent of the buoyancy frequency $\mathcal{N}$. This is consistent with the results that β_h is independent of $\mathcal{N}$, but does not trivially explain why β_h is

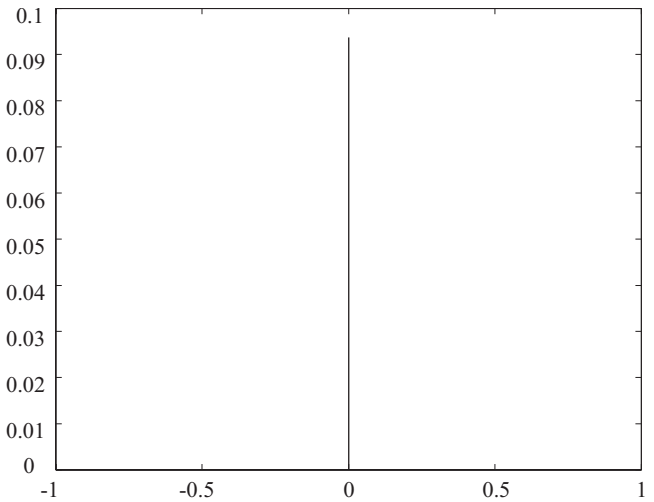

FIG. 5. pdf distribution of $L/u' \nabla \cdot \mathbf{u}$ in two-dimensional KS with $\psi=0$ case E in Table I.

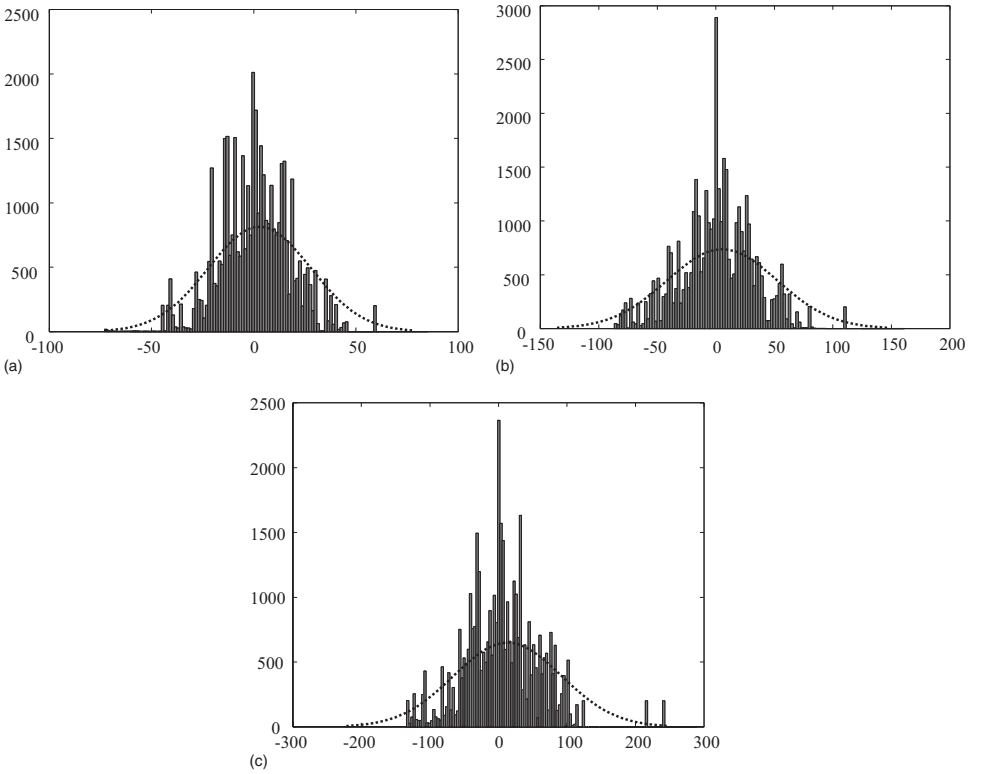

FIG. 6. pdf of $L/u'\nabla\cdot\mathbf{u}$ in two-dimensional compressible KS flow with (a) $\psi=\pi/16$, (b) $\pi/8$, and (c) π case E in Table I

smaller than β_{2D} rather than larger, in particular because the pdf of the horizontal velocity divergence is not skewed towards convergence regions. Furthermore, it appears from our numerical experiment with compressible two-dimensional KS isotropic turbulence that a very significant compressibility would be required for β_h to reach the value it reaches in stratified turbulence. We therefore now attempt a different approach for explaining why $\beta_h < \beta_{2D}$.

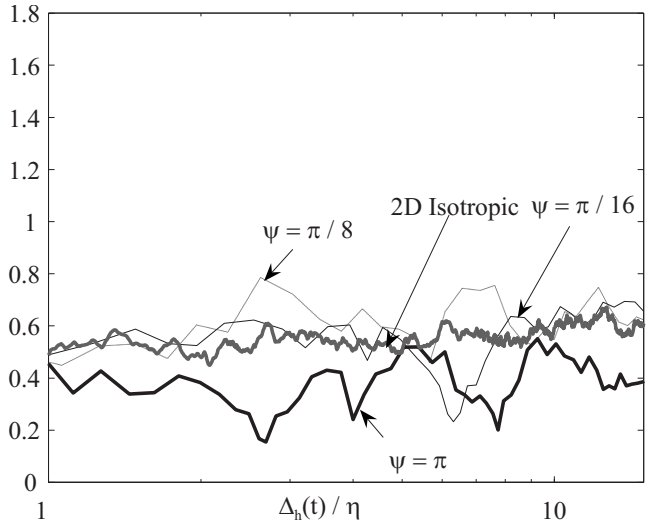

FIG. 7. β_{2D} for two-dimensional KS with different values of ψ case E in Table I.

V. TURBULENT PAIR DIFFUSION AND STAGNATION POINTS

A. Velocity definition stagnation points

In any reference frame $\mathfrak{F}$, at a given time t, locations $\mathbf{x}$ exist where the fluid velocity $u_i(\mathbf{x},t)$ vanishes. These locations vary with time, so that we can define $\mathbf{s}(t)=\mathbf{x}$ such that $u_i[\mathbf{s}(t),t]=0$ at each time. In order to track such zero-velocity points $\mathbf{s}(t)$ in time we must solve

$$u_i[s(0),0]=0,$$

$$\frac{d}{dt}u_i(\mathbf{s},t)=0. \tag{41}$$

In this paper we call stagnation points the solutions of Eq. (41). Considering a particular stagnation point $\mathbf{s}$ as a function of time, we can define a velocity $\mathbf{V}_s=(d/dt)\mathbf{s}(t)$ that describes its motion, and from Eq. (41) it comes

$$\frac{\partial u_i(\mathbf{s},t)}{\partial t}=-\mathbf{V}_s\cdot\nabla u_i(\mathbf{s},t). \tag{42}$$

By definition, the acceleration of a fluid particle is

$$a_i=\frac{\partial u_i}{\partial t}+\mathbf{u}\cdot\nabla u_i \tag{43}$$

and at $\mathbf{x}=\mathbf{s}(t)$, where $\mathbf{u}=0$, it follows from Eqs. (42) and (43) that the Lagrangian acceleration a_i of a fluid particle is

$$a_i = -\mathbf{V}_s \cdot \boldsymbol{\nabla} u_i. \tag{44}$$

This latter relation is purely kinematic and can be solved using Crammer's rule

$$\mathbf{V}_s = -\frac{[\det(\mathbf{a},\partial_2\mathbf{u},\partial_3\mathbf{u}),\det(\partial_1\mathbf{u},\mathbf{a},\partial_3\mathbf{u}),\det(\partial_1\mathbf{u},\partial_2\mathbf{u},\mathbf{a})]}{\det(\partial_1\mathbf{u},\partial_2\mathbf{u},\partial_3\mathbf{u})}, \tag{45}$$

where $\partial_j = \partial/\partial x_j$. This allows us to forgo the complicated process of not only having to find the stagnation points in the flow but also to track their trajectories in a time-dependent flow field. Indeed, only a snapshot of the flow field is necessary to determine the stagnation point velocity with Eq. (45).

Equation (44) can be used to find the order of magnitude of the r.m.s. values of the Lagrangian acceleration $a^\star$ at the stagnation points. We can expect the spatial derivative of the velocity to be dominated by the smallest length scale η or its analogous in KS, so that

$$\boldsymbol{\nabla} u_i \sim \frac{u_\eta}{\eta},$$

where u_η is the characteristic velocity fluctuation at η and

$$a^\star \sim V_s^\star \frac{u_\eta}{\eta}, \tag{46}$$

where $V_s^\star$ is the r.m.s. of V_s. In Eq. (46), $a^\star$ is calculated by averaging over all the stagnation points in the frame $\mathfrak{F}$ and is therefore equal to $a_l^\star$ the r.m.s. value of the local acceleration, $\mathbf{a}_l \equiv (\partial/\partial t)\mathbf{u}$, averaged over all the stagnation points. Later in this section we verify in kinematic simulation the validity of Eq. (46) with $a^\star$ replaced by $a_l^\star$ and we also test whether Eq. (46) remains valid for a' the r.m.s. of the Lagrangian acceleration calculated by averaging over the entire flow. If we assume the small scale velocity to scale as $u_\eta \sim (\epsilon\eta)^{1/3}$ and $\epsilon \sim u'^3/L$, then a normalised form for Eq. (46) is

$$\frac{La_l^\star}{u'^2} \sim \left(\frac{V_s^\star}{u'}\right)\left(\frac{L}{\eta}\right)^{2/3}. \tag{47}$$

In KS isotropic turbulence where large scale sweeping of small scales is absent, we can expect a Kolmogorov scaling for a_l', i.e., $a_l' \sim u_\eta^2/\eta$, which implies

$$\frac{La_l'}{u'^2} \sim \left(\frac{L}{\eta}\right)^{1/3} \tag{48}$$

and we can also expect $a^\star \sim u_\eta^2/\eta$ when $a^\star$ is calculated by averaging over stagnation points as, such averaging, removes the sweeping effect from acceleration statistics. So that

$$\frac{La_l^\star}{u'^2} \sim \left(\frac{L}{\eta}\right)^{1/3}. \tag{49}$$

From Eqs. (49) and (47) it follows that

TABLE II. KS parameters common to all runs in Sec. V.

N	number of modes	100
N_R	number of KS flow field realizations	1
N_a	number of sampling points per realization	10^6
u'	r.m.s. of the velocity fluctuation	1 m s^{-1}

$$\frac{V_s^\star}{u'} \sim \left(\frac{L}{\eta}\right)^{-1/3}. \tag{50}$$

The negative exponent in the scaling of $V_s^\star/u'$ implies that, in a statistical sense, the movement of the stagnation points becomes less significant when compared with the movement of the fluid particles (this latter characterized by u') as the Reynolds number increases. In that sense, the stagnation points become more persistent in space as explained in Refs. [9,15].

However, if there is a strong stratification, we expect $a' \sim \mathcal{N}u'$ when both conditions $L/\eta \gg 1$ and $\mathrm{Fr}_\eta \ll 1$ are satisfied as they imply that $\mathcal{N}u' \gg \mathcal{N}u_\eta \gg u_\eta^2/\eta \gg u'^2/L$ [using $u_\eta \sim u'(\eta/L)^{1/3}$]. This simply means that the buoyancy force dominates a' in strongly stratified turbulence. In the next section, this relation is tested and compared with isotropic turbulence acceleration scaling.

B. Scaling of the acceleration

For all the KS in Sec. V we chose the main computation parameters as in Table II Other parameters are in Table III

TABLE III. Flow parameters for the isotropic cases used in Sec. V.

case	$1/\eta$	L	$\mathcal{N}$	λ
Iso1	1000	0.01	0	0.5
	1000	0.1	0	0.5
	1000	0.5	0	0.5
	1000	1	0	0.5
	1000	10	0	0.5
	1000	100	0	0.5
	1000	1000	0	0.5
Iso3	100	0.1	0	0.5
	100	1	0	0.5
	100	5	0	0.5
	100	10	0	0.5
case	$1/\eta$	L	$\mathcal{N}$	λ
Iso2	1000	0.01	0	5
	1000	0.1	0	5
	1000	0.5	0	5
	1000	1	0	5
	1000	10	0	5
	1000	100	0	5
	1000	1000	0	5
Iso4	10	1	0	0.5
	500	1	0	0.5

TABLE IV. Flow parameters for the stratified cases used in Sec. V.

case	$1/\eta$	L	$\mathcal{N}$	λ
Stra1	100	0.1	1000	0.5
	100	1	1000	0.5
	100	10	1000	0.5
	100	100	1000	0.5
	100	1000	1000	0.5
	100	10000	1000	0.5
Stra2	100	1	varied	0.5
case	$1/\eta$	L	$\mathcal{N}$	λ
stra3	100	0.1	500	0.5
	100	1	500	0.5
	100	5	500	0.5
	100	10	500	0.5
stra4	10	1	500	0.5
	500	1	500	0.5
	1000	1	500	0.5
stra5	100	1	varied	0.5

for isotropic flows and in Table IV for stratified flows.

We split the acceleration into a local component $\mathbf{a}_l = \partial\mathbf{u}/\partial t$, and a convective component $\mathbf{a}_c = \mathbf{u}\cdot\boldsymbol{\nabla}/\mathbf{u}'$; and calculate both components in the frame $\mathfrak{F}_0$ defined as the frame where $\langle\mathbf{u}\rangle = 0$ and consequently also $\langle\mathbf{V}_s\rangle = 0$ (see Ref. [15]). $\mathbf{a}_l$ and $\mathbf{a}_c$ are obtained using the KS velocity field and its derivatives. The results for the scaling of the r.m.s. values of the local and convective accelerations, respectively, a_l' and a_c' in three-dimensional isotropic KS turbulence, are presented in Fig. 8. One can see that the scaling of the r.m.s. convective acceleration component is

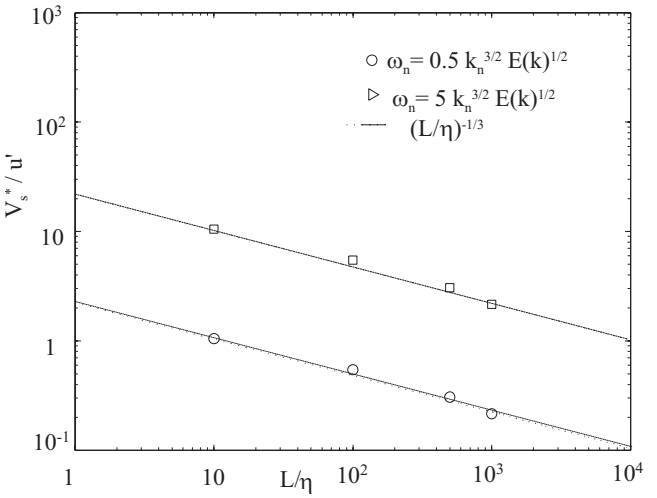

FIG. 9. r.m.s. of the stagnation point velocity $V_s^\star$ as a function of L/η. The two lines correspond to $(L/\eta)^{-1/3}$. (Cases Iso1 and Iso2 in Table III.)

$$\frac{La_c'}{u'^2} \sim \left(\frac{L}{\eta}\right)^{2/3}. \tag{51}$$

In contrast, the r.m.s. of the local acceleration a_l' scales as

$$\frac{La_l'}{u'^2} \sim \left(\frac{L}{\eta}\right)^{1/3}. \tag{52}$$

At stagnation points, the convective acceleration $\mathbf{a}_c$ is by definition equal to zero. Thus assuming $a_l^\star = a_l'$, from Eq. (50) it comes that the r.m.s. of the stagnation point velocities scales as $(L/\eta)^{-1/3}$ in isotropic KS turbulence (see Fig. 9). Figure 9 shows $V_s^\star/u'$ as a function of L/η where V_s is determined directly using Eq. (45) on the three-dimensional isotropic KS for cases Iso1 and Iso2 in Table III. We find the scaling derived in Eq. (50) which confirms the validity of our approach.

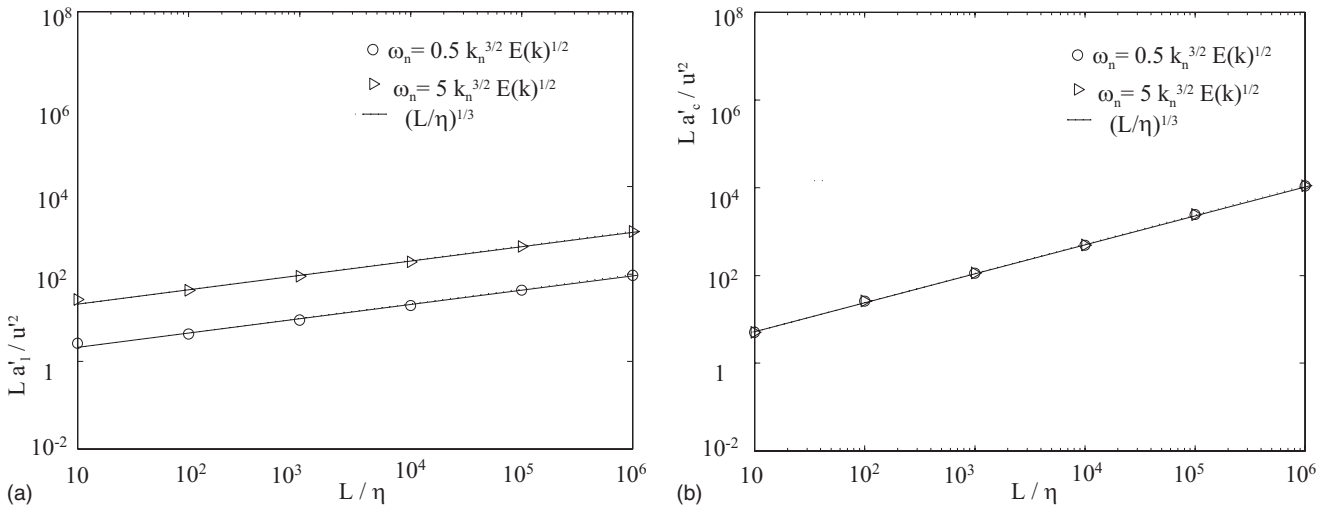

FIG. 8. Scaling with L/η of the r.m.s. values of (a) the local acceleration component a_l and (b) the convective acceleration component a_c. The flow parameters are detailed in Table III case Iso1 and Iso2). Averages are taken over the entire flow.

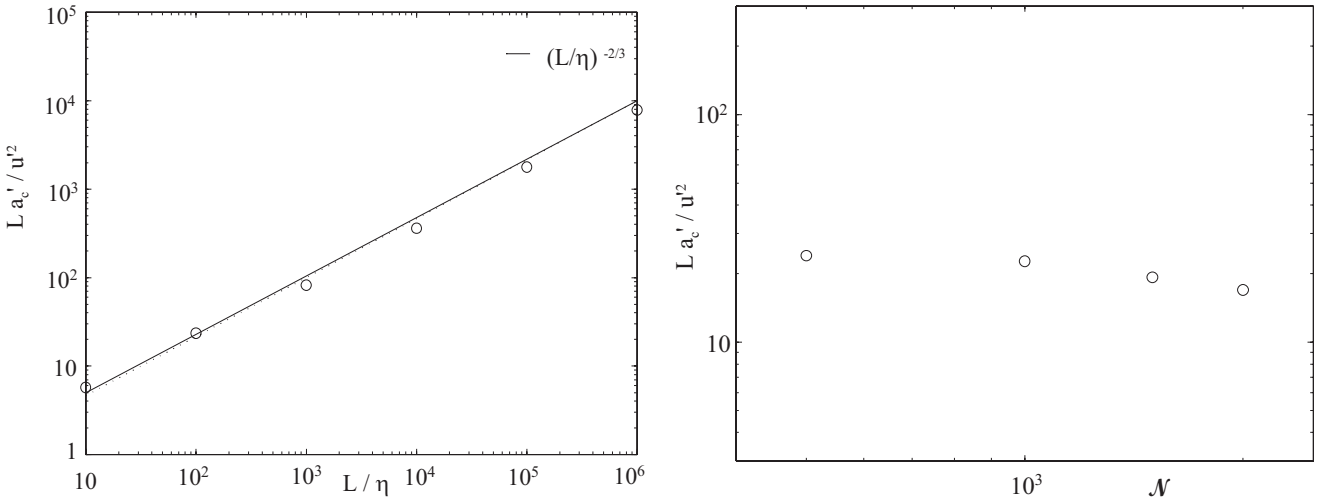

FIG. 10. r.m.s. of the convective acceleration a_c' for a stratified flow, $u'=1$ (a) a_c as a function of L/η for $\mathcal{N}=1000$; (b) a_c as a function of $\mathcal{N}$ for $L/\eta=100$.

In Figs. 8 and 9 the unsteadiness term ω_n in the KS has been varied, two values of λ, namely, 0.5 and 5 are compared. a_c' dominates a_l' when $\lambda=0.5$. Whereas, when $\lambda=5$, a_c' does not begin to dominate a_l' until $L/\eta>10^3$, which explains the total acceleration's scaling towards a more Kolmogorov-like scaling $[La'/u'^2\sim(L/\eta)^{1/3}]$ when $L/\eta \leqslant 10^3$, as also argued in and in agreement with Ref. [8].

C. Effect of stratification on the scaling of stagnation points

The rms of the convective (a_c') and local (a_l') accelerations (averages taken over all space) of stratified turbulence are presented, respectively, in Figs. 10 and 11. From Fig. 10 it is clear that the convective component of the acceleration scales with L/η as

$$a_c' \sim \frac{u'^2}{L}\left(\frac{L}{\eta}\right)^{2/3} \tag{53}$$

and is independent of $\mathcal{N}$. This is the same scaling as for the isotropic KS turbulence. However, from Fig. 11, the r.m.s. of the local acceleration in presence of stratification scales with $\mathcal{N}$ only:

$$a_l' \sim \mathcal{N}u'. \tag{54}$$

At stagnation points $a_c'=0$ and in our KS we have $\mathrm{Fr}_\eta \ll 1$, that is,

$$\mathcal{N}u' \gg \frac{u'^2}{L}\left(\frac{L}{\eta}\right)^{2/3} \tag{55}$$

then it follows from comparing Eq. (53) and Eq. (54) that in a KS with stratification, the r.m.s. of the acceleration is dominated by the local acceleration

$$a' \sim a_l'$$

and from Eq. (47)

$$\frac{La_l^\star}{u'^2} \sim \left(\frac{V_s^\star}{u'}\right)\left(\frac{L}{\eta}\right)^{2/3}. \tag{56}$$

That is, using Eq. (54)

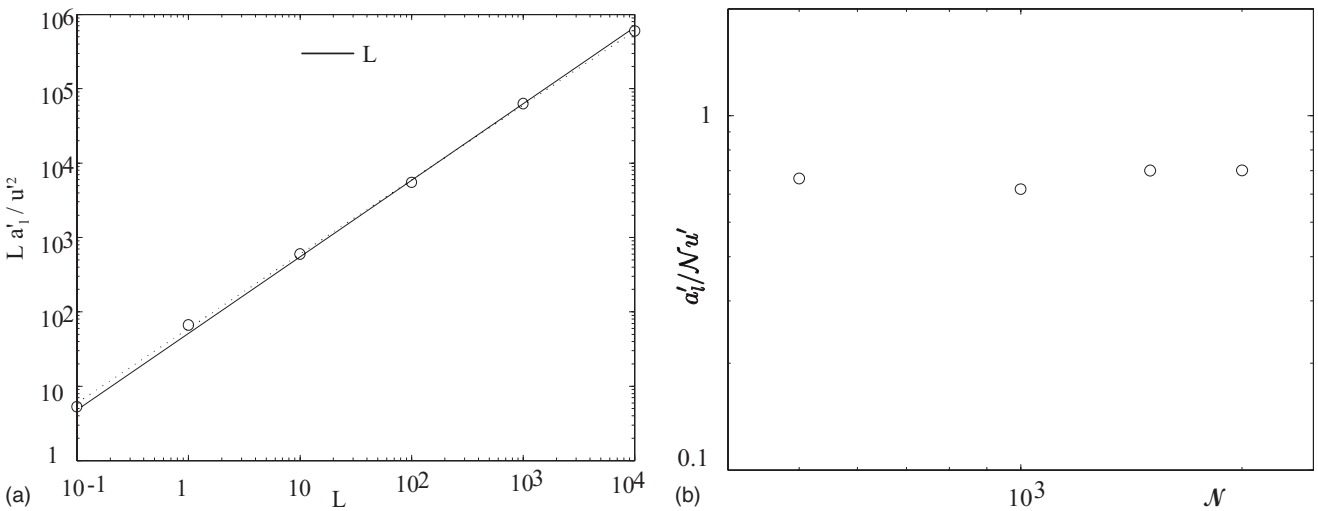

FIG. 11. Local acceleration component a_l, $u'=1$. (a) La_l'/u' as a function of L for $\mathcal{N}=1000$ and $\eta=0.01$; (b) $a_l'/\mathcal{N}u'$ as a function of $\mathcal{N}$ for $L/\eta=100$.

$$V_s^\star \sim \mathcal{N}L\left(\frac{L}{\eta}\right)^{-2/3} = u'\mathrm{Fr}^{-1}\left(\frac{L}{\eta}\right)^{-2/3} = u'\mathrm{Fr}_\eta^{-1}. \quad (57)$$

Figures 12(a)–12(c) show, respectively, $V_s^\star$, $V_{sh}^\star$, and $V_{sv}^\star$ as functions of L, clearly they scale with $LL^{-2/3}$. Figures 12(d)–12(f) show, respectively, $V_s^\star$, $V_{sh}^\star$, and $V_{sv}^\star$ as functions of η, clearly they scale with $(1/\eta)^{-2/3}$. Finally, Figs. 12(g)–12(i), show, respectively, $V_s^\star$, $V_{sh}^\star$, and $V_{sv}^\star$ as a functions of Fr_η and clearly they scale with Fr_η^{-1}. So that we can conclude that relation (57) is verified in KS.

Furthermore, Fig. 12 also shows more precisely that horizontal and vertical r.m.s. for the stagnation point velocities $V_{sh}^\star$ and $V_{sv}^\star$ scale as $\mathcal{N}L(L/\eta)^{-2/3}$ in strongly stratified turbulence. According to the condition $\mathrm{Fr}_\eta \ll 1$—where $\mathrm{Fr}_\eta = u_\eta/\eta\mathcal{N} = \mathrm{Fr}(L/\eta)^{2/3}$—the r.m.s. velocity of the stagnation points $V_s^\star$ is larger in stratified turbulence than $V_s^\star$ in isotropic turbulence for the same u', L and η. Furthermore, $V_s^\star$ is larger than u' in stratified turbulence when $\mathrm{Fr}_\eta \ll 1$. Therefore, fluid particles of stratified turbulence have less chances to meet and stay in the neighborhood of stagnation points, which have high curvature streamlines around them. This may suggest, but not conclusively, a depletion of turbulent pair diffusion in stratified turbulence compared to isotropic turbulence.

D. Number of stagnation points in stratified turbulence

In this section we compare the number of stagnation points in isotropic turbulence and in strongly stratified turbulence in order to further investigate the depletion of the horizontal pair diffusion in stratified turbulence. We use the multidimensional root finding method (Newton-Raphson method in Ref. [16]) to find all the stagnation points. This is an iterative method that requires initial points to start the iteration process. These initial points are separated by a distance δ smaller than η, and evenly distributed on a cube of side length L as shown in Fig. 13. We assume that each small box of size δ can only have one stagnation point and ignore points located outside the box of length L. We use a box-counting algorithm, and to avoid double counting of stagna-

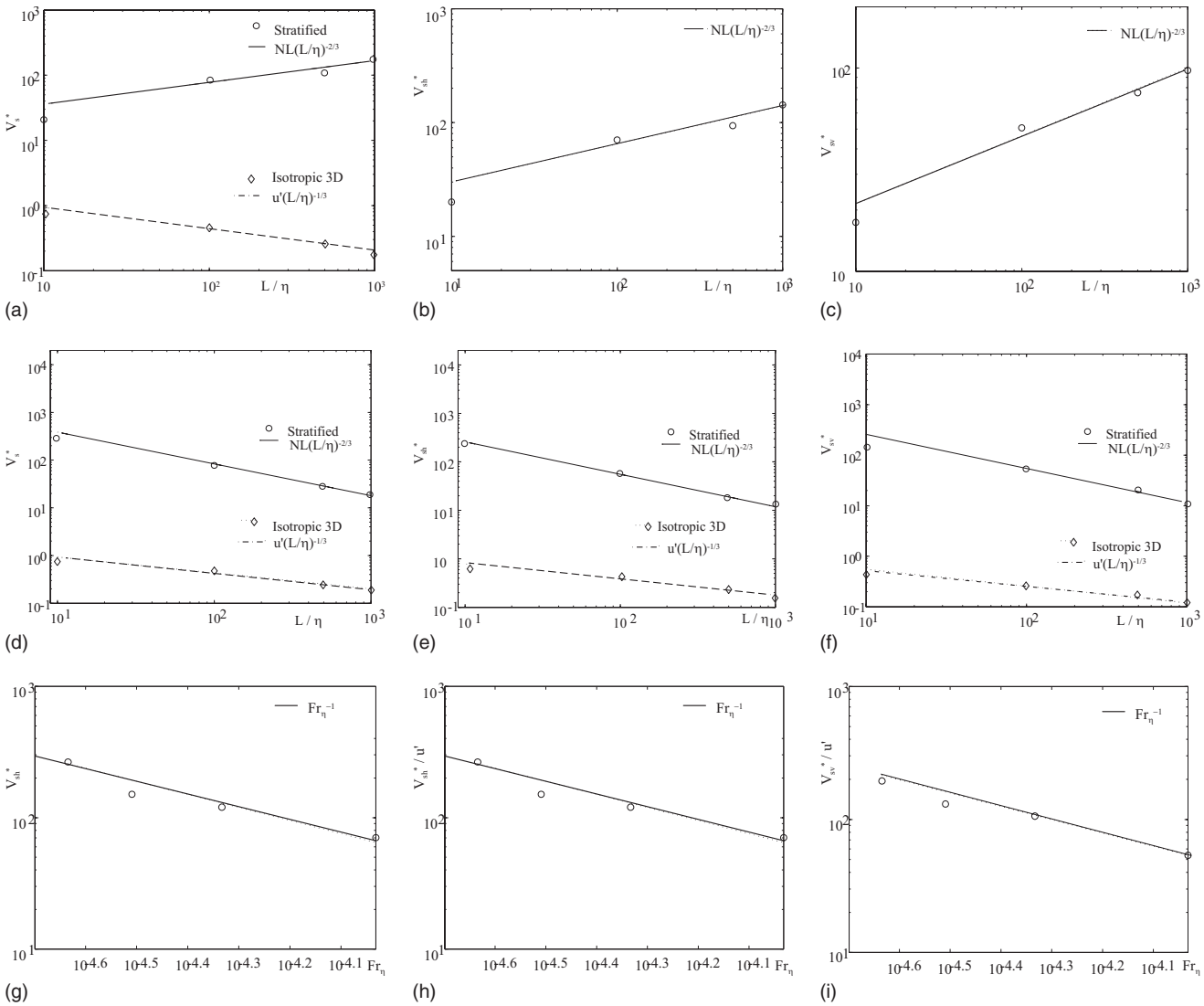

FIG. 12. r.m.s. velocity of the stagnation points in isotropic and stratified turbulence $u'=1$. (a)–(c) $\mathcal{N}=0$ and 500, and $1/\eta=100$, varying L. (d)–(f) $\mathcal{N}=0$ and 500, and $L=1$, varying η. (g)–(i) $L/\eta=100$, $L=1$, and varying Fr_η.

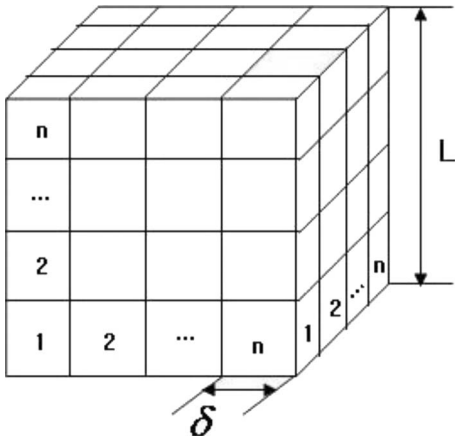

FIG. 13. Three-dimensional space split into small boxes of size δ.

tion points each box is only counted once. In order to reduce computing time, we also ignore stagnation points found beyond a distance $L/3$ from the starting point, because these stagnation points can be found from other starting points closer to them. For each Reynolds number, we calculate and plot n_s the number of stagnation points in the volume L^3 as a function of L/η for different buoyancy frequencies. The relation is well fitted by Eq. (58) with $D_s=2$ (see Fig. 14):

$$n_s \approx C_s\left(\frac{L}{\eta}\right)^{D_s}, \tag{58}$$

where C_s is a dimensionless parameter. This relation was derived by Ref. [16] and validated on data from KS and direct numerical simulation (DNS) of isotropic three-dimensional turbulence. We can then conclude that in KS, the Buoyancy frequency does not affect the number of stagnation points in comparison to an isotropic turbulence (see Fig. 14). This may be seen consistent with Fig. 2 which shows that β_h does not change as buoyancy frequency changes. Though, it does not help explaining why β_h is in

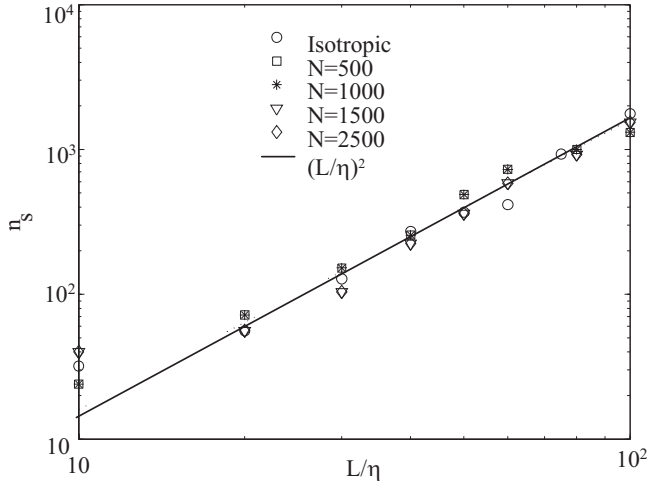

FIG. 14. Number of stagnation points per unit volume as a function of L/η in KS for different buoyancy ($L=1$) frequencies.

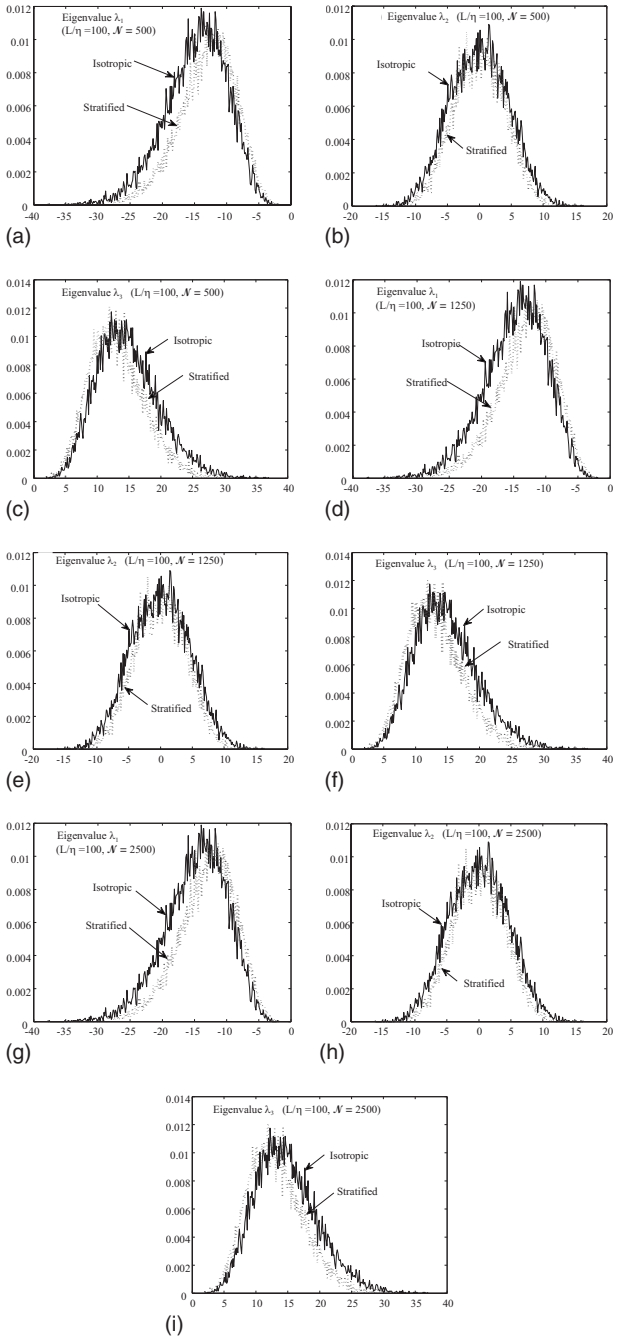

FIG. 15. p.d.f of the eigenvalues λ_1, λ_2, and λ_3 of straining rate at stagnation points in isotropic and stratified turbulence. λ_1 and λ_2 are for the horizontal component and λ_3 is for the vertical component.

stratified KS turbulence smaller than in two-dimensional isotropic KS turbulence.

However, it may explain why $(d/dt)\langle\Delta_h^2(t)\rangle \sim \langle\Delta_h^2\rangle^{2/3}$ is still valid in stratified turbulence as the arguments of Ref. [1] still hold because the buoyancy frequency does not affect D_s. Reference [1] introduced the idea of a geometrical separation process, as follows:

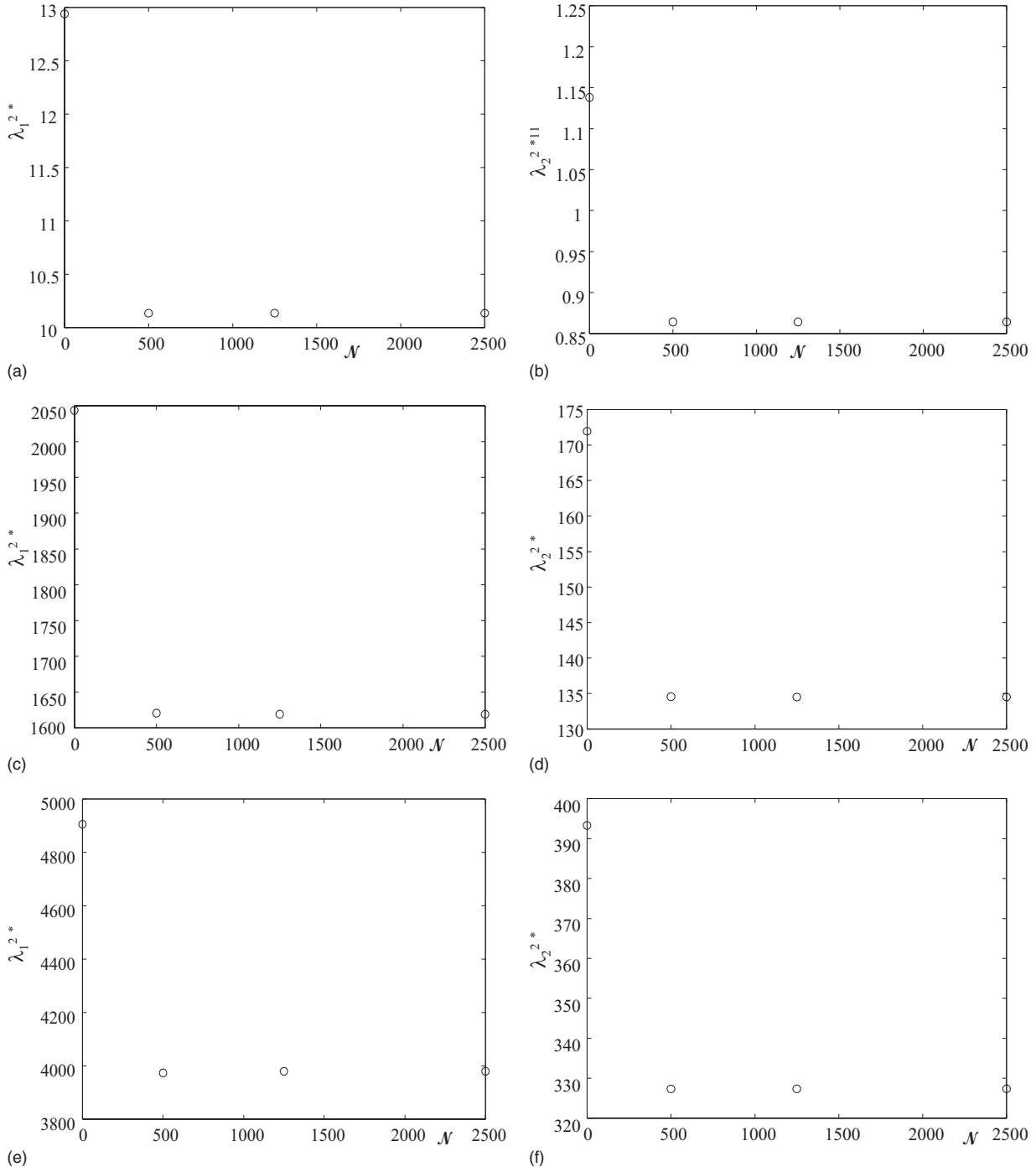

FIG. 16. Mean square eigenvalues of horizontal straining rate in isotropic ($\mathcal{N}=0$) and stratified turbulence with different L/η: (a) $\lambda_1^{2\star}$, $L/\eta=10$, (b) $\lambda_2^{2\star}$, $L/\eta=10$, (c) $\lambda_1^{2\star}$, $L/\eta=500$, (d) $\lambda_2^{2\star}$, $L/\eta=500$, (e) $\lambda_1^{2\star}$, $L/\eta=1000$, (f) $\lambda_2^{2\star}$, $L/\eta=1000$.

$$\Delta_0 \overset{T_\xi(\Delta_0)}{\rightarrow} \xi\Delta_0 \overset{T_\xi(\xi\Delta_0)}{\rightarrow} \xi^2\Delta_0 \overset{T_\xi(\xi^2\Delta_0)}{\rightarrow} \cdots, \tag{59}$$

where Δ_0 is the initial separation, ξ a constant multiplier, and $T_\xi(\xi^n\Delta_0)$ the characteristic time needed for pair separations to increase from $\xi^n\Delta_0$ to $\xi^{n+1}\Delta_0$. This characteristic time $T_\xi(\Delta)$ can be expressed as follows:

$$T_\xi(\Delta) \sim \frac{l_s}{u'} \sim \frac{n_s^{-1/3}}{u'}, \tag{60}$$

where l_s is the mean distance between stagnation points and n_s is the number of stagnation points per unit volume evaluated at L/Δ, i.e., $n_s(L/\Delta)$ [see Eq. (58)]. Let us suppose that at time t the pair separation is $\Delta=\xi^n\Delta_0$, then, using Eq. (58) it comes

$$t = \sum_{j=0}^{n-1} T_\xi(\xi^j \Delta_0) \sim \sum_{j=0}^{n-1} \frac{L}{u'}(\xi^j \Delta_0)^{D_s/3} \sim \frac{L}{u'} \Delta_0^{D_s/3} \frac{\xi^{D_s n/3} - 1}{\xi^{D_s/3} - 1} \tag{61}$$

which can be inverted to give

$$\langle \Delta^2 \rangle \sim L^2 \left(\frac{tu'}{L} \right)^{6/D_s}. \tag{62}$$

From our observation that $D_s = 2$ in stratified turbulence, it follows that

$$\langle \Delta^2 \rangle \sim t^3. \tag{63}$$

Using the fact that $\langle \Delta^2 \rangle = \langle \Delta_h^2 \rangle + \langle \Delta_3^2 \rangle$ and that $\langle \Delta_3^2 \rangle \ll \langle \Delta_h^2 \rangle$ in stratified flows [4], we can conclude that $\langle \Delta_h^2 \rangle \sim t^3$ which implies that $(d/dt)\langle \Delta_h^2(t) \rangle \sim \langle \Delta_h^2 \rangle^{2/3}$ (see, e.g., Ref. [8]).

VI. STRAINING RATE AND RICHARDSON'S COEFFICIENT

As counting the number of stagnation points in three-dimensional space does not explain the depletion of horizontal pair diffusion. We try a different approach based on the study of the strain rate.

KSs having by construction no energy cascade dynamics, we venture to interpret $\langle \Delta^2 \rangle \simeq G_\Delta \epsilon t^3$ as being in fact

$$\langle \Delta^2 \rangle \simeq G_\Delta \{ 2\nu \langle S^2 \rangle \} t^3, \tag{64}$$

where we used the kinematic relation $\epsilon = 2\nu \langle S^2 \rangle$ between ϵ and $\langle S^2 \rangle = \langle S_{ij} S_{ji} \rangle$ with

$$S_{ij} = \frac{1}{2} \left(\frac{\partial u_j}{\partial x_i} + \frac{\partial u_i}{\partial x_j} \right). \tag{65}$$

There is no kinematic viscosity either in KS, but we can derive an implicit one from η and $\langle S^2 \rangle$ as follows:

$$\eta = \epsilon^{-1/4} \nu^{3/4} \sim \left(\frac{\nu^3}{\nu \langle S^2 \rangle} \right)^{1/4}, \tag{66}$$

i.e., $\nu \simeq C \eta^2 \langle S^2 \rangle^{1/2}$ where C is a dimensionless constant independent of all KS parameters. As a result, we can surmise that the Richardson law in KS should really be written as

$$\langle \Delta^2 \rangle \simeq G_\Delta 2\nu \langle S^2 \rangle t^3 \simeq 2 G_\Delta C \eta^2 (\langle S^2 \rangle^{1/2} t)^3, \tag{67}$$

which yields from the definition of β_h

$$\beta_h = \frac{3L^{1/3}}{u'} [2C\eta^2 \langle S^2 \rangle^{3/2}]^{1/3} G_{\Delta h}^{1/3}. \tag{68}$$

The observed reduction of β_h by strong stratification can therefore be directly linked to a reduction of $\langle S^2 \rangle$ by the same stratification. Any modification that a strong stratification may impose on $\langle S^2 \rangle^{1/2}$ is directly reflected on β_h.

To test this idea, we calculate the statistics of the straining rate [Eq. (65)], that is its r.m.s. and the distribution of the eigenvalues of S_{ij} at stagnation points. The stagnation points are regions which move more and more slowly with increasing L/η as shown in Sec. V B, so they can have an effect on the horizontal separation of fluid elements and thereby account for $\langle \Delta_h^2 \rangle \sim t^3$. However, their full effect, which includes their effect on β_h remains dependent on the local straining rate.

We define the three eigenvalues of the straining rate tensor such that $\lambda_1 \leqslant \lambda_2 \leqslant \lambda_3$. In order to verify incompressibility $\lambda_1 + \lambda_2 + \lambda_3 = 0$. Therefore, $\lambda_3 > 0$ and $\lambda_1 < 0$. Our KS calculations show that $|\lambda_1|$ and $|\lambda_3|$ are statistically smaller in strongly stratified turbulence than in isotropic turbulence (see Fig. 15).

Figure 16 shows the variance of two eigenvalues $\lambda_1^{2\star}$ and $\lambda_2^{2\star}$ (averages taken over stagnation points) as functions of $\mathcal{N}$ for different inertial ranges L/η. The variances are independent of $\mathcal{N}$. That can be the reason why β_h in stratified turbulence is also found independent of $\mathcal{N}$. From Kolmogorov's scaling, we get

$$\langle \omega^2 \rangle = 2\langle S^2 \rangle \sim \left(\frac{u'}{L} \right)^2 \left(\frac{L}{\eta} \right)^{4/3}, \tag{69}$$

where ω is the vorticity $(\nabla \times u)$. The mean square straining rate and vorticity of an isotropic and stratified turbulence follow the scaling $(L/\eta)^{4/3}$. We define the dimensionless constant C' as

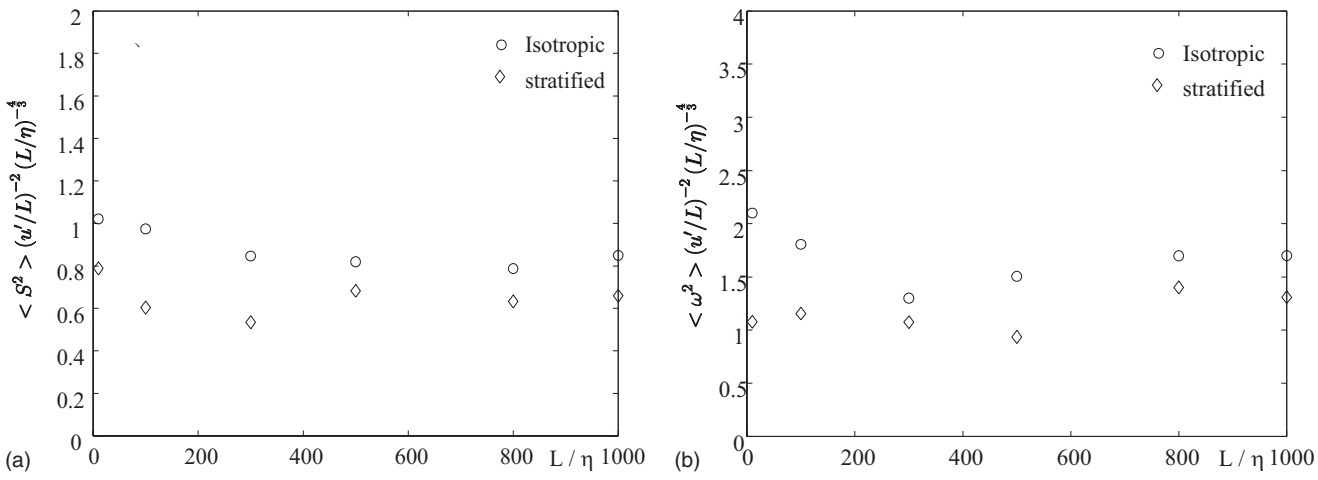

FIG. 17. Coefficient C' scaled mean square straining rate and vorticity of isotropic (○) and stratified (◇) turbulence.

TABLE V. KS parameters used in runs in Sec. VI.

N	number of modes	100
N_R	number of KS flow field realizations	1
N_a	number of sampling points per realization	10^6
u'	rms of the velocity fluctuation	1 m s^{-1}
Fig. 15	$L=1$ m, $L/\eta=100$	
Fig. 16	$L=1$ m	
Fig. 17	$L=1$ m, $\mathcal{N}=500$	

$$\langle \omega^2 \rangle = 2\langle S^2 \rangle = C' \left(\frac{u'}{L} \right)^2 \left(\frac{L}{\eta} \right)^{4/3} \tag{70}$$

and find that C' for the stratified turbulence is smaller than C' of isotropic turbulence. This is the main explanation for the observed depletion of horizontal pair diffusion in stratified turbulence. Figure 17 clearly shows that the enstrophy and the average square strain rate tensor are depleted in the presence of stratification, thus we conclude that the depletion of the horizontal pair diffusion in stratified turbulence can be understood as a depletion of the strain rate (see Table V).

VII. CONCLUSION

Though our results have been obtained with KS and are valid when our RDT-KS is valid that is in the limit of $\mathrm{Fr}_\eta = u_\eta / \eta \mathcal{N} < 1$. We have found that the probability density function of the horizontal divergence of the velocity field $(\boldsymbol{\nabla} \cdot \mathbf{u}_h)$ is not a Dirac distribution in the presence of stratification but a Gaussian symmetrically distributed around 0. This Gaussian does not depend on the Froude number and neither does the depletion of the horizontal pair diffusion. However, they both disappear in the absence of stratification, i.e., for an infinite Froude number.

We therefore sought to explain this depletion of the horizontal pair diffusion by vertical stratification in terms of the statistics of stagnation points in the line of the recent approach to Richardson pair diffusion by Refs. [9,15,16,1]. We measured the number of stagnation points (n_s) in the KS of three-dimensional strongly stratified turbulence and found that it was virtually identical to what it is in KS of three-dimensional isotropic turbulence.

The root mean square horizontal and vertical stagnation point velocities of stratified turbulence V'_{sh} and V'_{sv} scale with $\mathcal{N}L(L/\eta)^{-2/3}$ when $\mathrm{Fr}_\eta \ll 1$. Hence, they are both larger than u' and therefore also of their counterparts in isotropic turbulence which get progressively smaller than u' as L/η increasing. The strong stratification destroys the persistence of the stagnation points if non linear processes are not taken into account, as in KS.

The stratification does lead to a depletion of the average square strain rate tensor, as well as of all average square strain rate eigenvalues. We can conclude that it is these effects of stratification on the strain rate tensor that explain the depletion of the horizontal turbulent pair diffusion.

[1] In this paper, particles are synonymous with fluid elements.
[2] Y. Kimura and J. R. Herring, J. Fluid Mech. **328**, 253 (1996).
[3] F. S. Godeferd, N. A. Malik, C. Cambon, and F. Nicolleau, Appl. Sci. Res. **57**, 319 (1997).
[4] F. Nicolleau and J. C. Vassilicos, J. Fluid Mech. **410**, 123 (2000).
[5] Y. Kaneda and T. Ishida, J. Fluid Mech. **402**, 311 (2000).
[6] L. F. Richardson, Beitr. Phys. Atmos. **15**, 24 (1926).
[7] F. Nicolleau and G. Yu, Phys. Fluids **16**, 2309 (2004).
[8] F. Nicolleau, G. Yu, and J. C. Vassilicos, Fluid Dyn. Res. **40**, 68 (2008).
[9] D. R. Osborne, J. C. Vassilicos, K. Sung, and J. D. Haigh, Phys. Rev. E **74**, 036309 (2006).
[10] F. Nicolleau and G. Yu, Phys. Rev. E **76**, 066302 (2007).
[11] C. Cambon, F. S. Godeferd, F. Nicolleau, and J. C. Vassilicos, J. Fluid Mech. **499**, 231 (2004).
[12] J. C. H. Fung, J. C. R. Hunt, N. A. Malik, and R. J. Perkins, J. Fluid Mech. **236**, 281 (1992).
[13] F. S. Godeferd and C. Cambon, Phys. Fluids **6**, 2084 (1994).
[14] S. Goto, D. R. Osborne, J. C. Vassilicos, and J. D. Haigh, Phys. Rev. E **71**, 015301(R) (2005).
[15] J. Davila and J. C. Vassilicos, Phys. Rev. Lett. **91**, 144501 (2003).
[16] S. Goto and J. C. Vassilicos, New J. Phys. **6**, 65 (2004).